Furthermore, in previous phase I studies, HAI chemotherapy with GEM was well-tolerated up to 1,000 mg/m^2 infused over 400 min (8,9).

According to the pharmacokinetics of GEM, when 1,000 mg/m^2 of GEM is administered via intravenous infusion over 30 min, the average maximum plasma concentrations reach 21,865±4,165 ng/ml by 15 min. The flow volume of the hepatic artery proper is reportedly ~330 ml/min (11). When an 800-mg dose of GEM is infused into the hepatic artery proper over a 30-min period, the local plasma concentration in the liver reaches ~80,000 ng/ml by 30 min. Vogl *et al* (8) reported that the maximum tolerated dose of HAI chemotherapy with GEM was 1,400 mg/m^2. Conversely, the plasma concentration of 5-FU with a 250-mg infusion into the hepatic artery proper over a 24-h period was 0.5 µg/ml. This concentration is equal to that obtained following administration of 30 mg/kg (1,350 mg in the reported patient) of 5-FU over a 24-h period (23). In addition, Maruyama *et al* (24) reported that when 1,000-1,500 mg of 5-FU was infused into the hepatic artery over a period of 5 h, the maximum plasma concentration was 0.48 µg/ml on average, without the development of any grade 3 adverse effects. Super-selective HAI may deliver high doses of chemotherapeutic agents into the tumor vessels, producing increased regional levels with higher effectiveness and lower incidence/severity of systemic side effects. In this study, the response rate was 85.7%, despite 6 out of the 7 cases having received systemic chemotherapy with GEM prior to HAI. Moreover, no severe toxicity developed with this therapy. These findings indicate that HAI chemotherapy is safe and effective for the treatment of postoperative liver metastasis from pancreatic carcinoma. The drawbacks of HAI chemotherapy include problems with the catheter and the appearance of new lesions outside the liver. In this study, 6 out of the 7 cases eventually required removal of the HAI catheter and the subcutaneous implantable port system due to problems with the tube, and new lesions outside the liver appeared in all 7 patients. Even in the GEM+5-FU group, we performed HAI with GEM plus oral S-1 therapy after 10 cycles under the hypothesis of the appearance of extra-hepatic metastases. Moreover, patients who did not undergo R0 surgery for primary lesions and patients suspected of having extra-hepatic metastases were assigned to the GEM+S-1 group.

Although the safety of GEM plus S-1 therapy was previously demonstrated in the GEST trial (15), the occurrence of adverse events was greater in the phase I study of neoadjuvant chemotherapy (NAC) for resectable pancreatic cancer performed in our department. In addition, NAC with GEM plus S-1 was not well-tolerated (25). Nakahira *et al* (26) reported that pretreatment with S-1 enhances the GEM effects on pancreatic cancer xenografts. The mechanism underlying these enhanced effects is considered to be 5-FU-induced upregulation of human equilibrative nucleoside transporter 1, the major mediator of GEM cellular uptake. In our trial, S-1 was administered for 14 consecutive days prior to GEM, which may explain the greater number of adverse events observed in our study. However, to maximize the effect of GEM, it is recommended that S-1 be administered prior to GEM. By using a combination of oral S-1 and HAI of GEM, effective amounts of the two chemotherapeutic agents were reached in the liver and the systemic side effects were reduced.

In conclusion, HAI chemotherapy is safe and effective for the treatment for postoperative metastases from pancreatic cancer confined to the liver. A clinical phase I trial of HAI chemotherapy with GEM plus 5-FU or oral S-1 is currently being undertaken, which includes the measurement of GEM concentration in the peripheral blood of patients in order to determine the optimal dose.

References

1. International Agency for Research on Cancer, World Health Organization. Globocan 2008. World Health Organization Website. http://globocan.iarc.fr/. Accessed October 1, 2010.
2. Ishii H, Furuse J, Boku N, *et al*: Phase II study of gemcitabine chemotherapy alone for locally advanced pancreatic carcinoma: JCOG0506. Jpn J Clin Oncol 40: 573-579, 2010.
3. Evans DB, Abbruzzese JL and Willett CG: Cancer of the pancreas. In: Cancer: Principles and Practice of Oncology. De Vita VT, Hellman S, Rosenberg SA (eds). 6th edition. Lippincott Williams and Wilkins, Philadelphia, pp1126-1161, 2001.
4. Oettle H, Post S, Neuhaus P, *et al*: Adjuvant chemotherapy with gemcitabine vs. observation in patients undergo curative-intent resection of pancreatic cancer: a randomized controlled trial. JAMA 297: 267-277, 2007.
5. Aloia TA, Lee JE, Vauthey JN, *et al*: Delayed recovery after pancreaticoduodenectomy: a major factor impairing the delivery of adjuvant chemotherapy? J Am Coll Surg 204: 347-355, 2007.
6. Sandy H, Bruckner H, Cooperman A, Paradiso J and Kiefer L: Survival advantage of combined chemoradiotherapy compared with resection as the initial treatment of patients with regional pancreatic carcinoma. An outcomes trial. Cancer 89: 314-327, 2000.
7. Ensminger WD, Rosowsky A and Raso V: A clinical pharmacological evaluation of hepatic arterial infusions of 5-fluoro-2-deoxyuridine and 5-fluoroufacil. Cancer Res 38: 3784-3792, 1978.
8. Vogl TJ, Schwarz W, Eichler K, *et al*: Hepatic intraarterial chemotherapy with gemcitabine in patients with unresectable cholangiocarcinoma and liver metastases of pancreatic cancer: a clinical study on maximum tolerable dose and treatment efficacy. J Cancer Res Clin Oncol 132: 745-755, 2006.
9. Tse AN, Wu N, Patel D, Haviland D and Kemeny N: A phase I study of gemcitabine given via intrahepatic pump for primary or metastatic hepatic malignancies. Cancer Chemother Pharmacol 64: 935-944, 2009.
10. Van Riel JM, Peters GJ, Mammatas LH, *et al*: A phase I and pharmacokinetic study of gemcitabine given by 24-h hepatic arterial infusion. Eur J Cancer 45: 2519-2527, 2009.
11. Tajima H, Ohta T, Kitagawa H, *et al*: Pilot study of hepatic arterial infusion chemotherapy with gemcitabine and 5-fluorouracil for patients with postoperative liver metastases from pancreatic cancer. Exp Therap Med 2: 265-269, 2011.
12. Nakamura K, Yamaguchi T, Ishihara T, *et al*: Phase I trial of oral S-1 combined with gemcitabine in metastatic pancreatic cancer. Br J Cancer 92: 2134-2139, 2005.
13. Ueno H, Okusaka T, Ikeda M, *et al*: A phase I study of combination chemotherapy with gemcitabine and oral S-1 for advanced pancreatic cancer. Oncology 69: 421-427, 2005.
14. Nakamura K, Yamaguchi T, Ishihara T, *et al*: Phase II trial of oral S-1 combined with gemcitabine in metastatic pancreatic cancer. Br J Cancer 94: 1575-1579, 2006.
15. Ueno H, Ioka T, Ikeda M, *et al*: Randomized phase III study of gemcitabine plus S-1 (GS) versus S-1 alone, or gemcitabine alone in patiens with locally advanced and metastatic pancreatic cacer in Japan and Taiwan: GEST study. J Clin Oncol 31: 1640-1648, 2013.
16. Urata K, Kawasaki S, Matsunami T, *et al*: Calculation of child and adult standard liver volume for liver transplantation. Hepatology 21: 1317-1321, 1995.
17. Tajima H, Ohta T, Kitagawa H, *et al*: Hepatic arterial infusion chemotherapy for post-operative liver metastases from pancreatic cancer in a patient with leukocytopenia: a case report. Exp Therap Med 1: 987-990, 2010.
18. Therasse P, Arbuck SG, Eisenhauer EA, *et al*: New guidelines to evaluate the response to treatment in solid tumors. European Organization for Research and Treatment of Cancer, National Cancer Institute of the United States. National Cancer Institute of Canada. J Natl Cancer Inst 92: 205-216, 2000.

19. Nagakawa T, Nagamori M, Futakami F, *et al*: Result of extensive surgery for pancreatic carcinoma. Cancer 77: 640-645, 1996.
20. Noto M, Miwa K, Kitagawa H, *et al*: Pancreas head carcinoma: frequency of invasion to soft tissue adherent to the superior mesenteric artery. Am J Surg Pathol 29: 1056-1061, 2005.
21. Homma H, Akiyama T, Mezawa S, *et al*: Advanced pancreatic carcinoma showing a complete response to arterial infusion chemotherapy. Int J Clin Oncol 9: 197-201, 2004.
22. Miyanishi K, Ishiwatari H, Hayashi T, *et al*: A Phase I trial of arterial infusion chemotherapy with gemcitabine and 5-fluorouracil for unresectable advanced pancreatic cancer after vascular supply distribution via superselective embolization. Jpn J Clin Oncol 38: 268-274, 2008.
23. Kikuchi K and Kanno H: Comparison for blood levels and clinical effects between tablet and other dosage forms of 5-fluorouracil (5-FU). Gan To Kagaku Ryoho 6: 559-565, 1979 (In Japanese).
24. Maruyama S, Ando M and Watayo T: Concentration of 5-FU after hepatic artery infusion chemotherapy for liver metastases of colorectal cancer. Gan To Kagaku Ryoho 30: 1635-1638, 2003 (In Japanese).
25. Tajima H, Kitagawa H, Tsukada T, *et al*: A phase I study of neoadjuvant chemotherapy with gemcitabine plus oral S-1 for resectable pancreatic cancer. Mol Clin Oncol 1: 768-772, 2013.
26. Nakahira S, Nakamori S, Tsujie M, *et al*: Pretratment with S-1, an oral derivative of 5-fluorouracil, enhances gemcitabine effect in pancreatic cancer xenografts. Anticancer Res 28: 179-186, 2008.

Published OnlineFirst August 20, 2014; DOI: 10.1158/1535-7163.MCT-14-0151

Cancer Biology and Signal Transduction

Molecular Cancer Therapeutics

Longitudinal Time-Dependent Effects of Irradiation on Multidrug Resistance in a Non–Small Lung Cancer Cell Line

Yumiko Kono, Keita Utsunomiya, Shohei Kanno, and Noboru Tanigawa

Abstract

Multidrug resistance (MDR) in cancer is known to decrease the therapeutic efficacy of chemotherapy. The effects of irradiation on MDR in cancer cells remain unclear. Tc-99m methoxyisobutylisonitrile (MIBI) exhibits the same ATP-binding cassette (ABC) transporter kinetics as the chemotherapeutic compound doxorubicin. In this study, we investigated the synergistic effects of chemotherapeutics and irradiation [0 Gy: C (control) group; 3, 6, 9, 12 Gy: I (irradiation) group] in the human non–small lung cancer cell line H1299 exhibiting MDR, on MIBI and doxorubicin ABC transporter kinetics, *in vitro* and *in vivo*, respectively. *In vitro*, inhibition of H1299 cell proliferation by irradiation was found to be irradiation dose dependent. The degree and duration of MDR inhibition *in vitro* in H1299 were also dose dependent. In the cells of both the C group and 3-Gy I group, no significant difference of MIBI accumulation was observed. In the 6-Gy I group, a higher MIBI accumulation was observed at only 7 days after irradiation relative to the C group. A higher MIBI accumulation in the 9- and 12-Gy I groups with a significant difference from the C group was observed at 4 to 14 days after irradiation. A significant negative correlation between intracellular MIBI accumulation and cell replication was found. *In vivo*, high accumulation and retention of doxorubicin were observed in irradiated tumors in the H1299 xenograft mice group at 4 to 14 days after 9-Gy irradiation compared with the control mice group. These results provide evidence for a synergistic effect of concurrent chemotherapy and radiotherapy. *Mol Cancer Ther; 13(11); 2706–12. ©2014 AACR.*

Introduction

Multidrug resistance (MDR) in cancer cells is known to decrease the therapeutic efficacy of some types of chemotherapy (1). MDR is due to the overexpression of ATP-binding cassette (ABC) transporters, such as P-glycoprotein (Pgp), multidrug resistance–associated protein 1 (MRP1), and others, in the plasma membrane. These overexpressed ABC transporters pump energy-dependent chemotherapeutic agents out from the intracellular volume into the extracellular milieu. MDR cancer cells thus exhibit resistance to chemotherapy resulting in poor outcomes for patients (2, 3).

Concurrent chemoradiotherapy has now been established as a standard treatment based on evidence of improved efficacy in treatment outcomes as compared with only radiation therapy (4–8). However, the response of various tumors to chemoradiotherapy can vary greatly, even for tumors of the same histologic type, for a given treatment regimen. Furthermore, some patients acquire MDR during their first course of chemotherapy, whereas others acquire MDR only during subsequent treatments. In addition, the irradiation protocols that should be used to obtain the greatest beneficial synergy with chemotherapy have not been determined to date.

In chemoradiotherapy, suppression of MDR is the key to increasing the efficacy of many chemotherapeutic agents. However, it should be also noted that with regard to effects of radiation on MDR in cancer cells there are conflicting reports. Some researchers have reported that irradiation inhibits MDR (9, 10), whereas other researchers have reported that irradiation promotes MDR (11). Further research is thus required to elucidate the effects of irradiation on MDR in specific tumor cell types.

Tc-99m hexakis-2-methoxyisobutylisonitrile (MIBI) is a nuclear medicine agent used in diagnostic imaging of the parathyroid and heart. MIBI, as a substrate for Pgp and MRP1, has been shown to have similar pharmacokinetics to chemotherapeutic agents such as doxorubicin (12–15). Therefore, there are a number of clinical research reports assessing the utility of MIBI in predicting the chemotherapeutic response in non–small cell lung cancer (16–23).

The purpose of this study is to investigate how to optimally combine chemotherapy and radiation therapy to achieve the maximum synergistic effect in

Department of Radiology, Kansai Medical University, Hirakata, Osaka, Japan.

Corresponding Author: Yumiko Kono, Kansai Medical University, 2-5-1, Shinmachi, Hirakata, Osaka, 573-1010, Japan. Phone: 81-72-804-0101; Fax: 81-72-804-2072; E-mail: kohnoy@hirakata.kmu.ac.jp

doi: 10.1158/1535-7163.MCT-14-0151

Published OnlineFirst August 20, 2014; DOI: 10.1158/1535-7163.MCT-14-0151

chemoradiotherapy. Using doxorubicin *in vivo* and MIBI *in vitro*, we investigated the relationship between multiplication and MDR of non–small lung cancer cells and the time-dependent effect of irradiation on MDR in non–small cancer cells.

Materials and Methods

Cell line and tracers

Human non–small lung cancer cells (H1299) transfected with the *wtp53* gene (H1299/*wtp53*), obtained in 2009 from the Division of Oncology, Biomedical Imaging Research Center, Fukui University, Japan, were used in this study. This cell line was cultured in medium containing Geneticin as a selective agent and was thus confirmed to be H1299/*wtp53*. MDR was demonstrated in the H1299 cells through immunostaining with Pgp and MRP-1 monoclonal antibodies (Fig. 1).

The radiotracer Tc-99m MIBI, a substrate of MDR-related ABC transporters, was used *in vitro* as a proxy for chemotherapeutic drugs. *In vivo*, the chemotherapeutic drug doxorubicin was used as a fluorescent tracer.

Cell culture and irradiation

H1299 cells were cultured at 37°C in a conventional humidified 5% CO_2 incubator. The cells were grown in DMEM containing 10% (v/v) FBS, streptomycin (50 μg/mL), and Geneticin (G418; 200 μg/mL). The single-cell suspensions, in a canister 105 mm in height and 312 mm in diameter, were γ-ray irradiated (Gammacell 40 Exactor; Nordion International) with a central dose rate of 0.84 Gy/min before cell seeding at room temperature. Five groups, categorized according to radiation dose, were prepared: 0 Gy (control group), 3 Gy (3-Gy group), 6 Gy (6-Gy group), 9 Gy (9-Gy group), and 12 Gy (12-Gy group). After irradiation, the cells were incubated for 1, 4, 7, or 14 days in tissue culture flasks according to the method described above.

Replication study *in vitro*

At each of 1, 4, 7, and 14 days after γ-ray irradiation, the I groups (3, 6, 9, and 12 Gy) and C group (0 Gy) were trypsinized, centrifuged, and resuspended in 0.5 to 2.0 × 10^6/225 cm^2 (0 and 3 Gy: 0.5 × 10^6/225 cm^2; 6 Gy: 1 × 10^6/225 cm^2; 9 and 12 Gy: 2 × 10^6/225 cm^2) flasks in fresh media to exclude the inhibitory effect by confluent. For the H1299 cell line, it was possible to subculture the highest-dose 12-Gy irradiation group in the same manner as the lower-dose groups.

The cell numbers were counted by staining with Trypan blue. For the 14 days incubation group, to prevent the cell cultures in the flasks from becoming confluent, the cells were subcultured into new flasks at 7 days after irradiation. The replication rate (RR) and replication coefficient (RC) at each time point after irradiation, 1, 4, 7, and 14 days, were calculated using the following equations:

$$RR = \frac{N}{N_0}, \quad RC = \frac{\log_2(N) - \log_2(N_0)}{t - t_0},$$

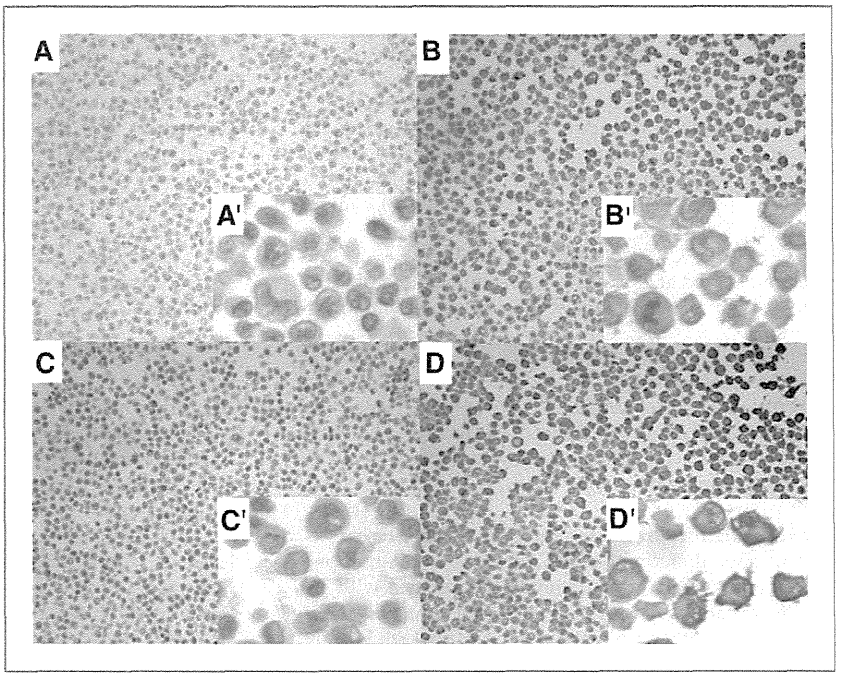

Figure 1. Immunostaining of Pgp and MRP-1 in H1299 cell line. Magnification: A, B, C, and D, ×40; A′, B′, C′, and D′, ×100. B and B′, H1299 expressed Pgp and isotype-matched negative control (A and A′). D and D′, H1299 also expressed MRP-1 and isotype-matched negative control (C and C′).

Published OnlineFirst August 20, 2014; DOI: 10.1158/1535-7163.MCT-14-0151

where N is the number of cells after irradiation, N_0 is the number of cells before irradiation, and $t - t_0$ is the number of days under culture.

The replication studies were repeated four times.

Tc-99m MIBI accumulation study *in vitro*

For the MIBI accumulation studies, cells in the C and I groups were trypsinized, after the end of the incubation period, and suspended in 7.0-mL complete medium at a concentration of 1.0 to 2.0 $\times$ 10^6 cells/mL. The cell suspensions were incubated at 37°C in a stirred water bath. Samples (300 μL) were obtained in duplicate at 1, 15, 30, 45, and 60 minutes after adding 370 kBq MIBI and transferred to 1.5-mL microcentrifuge tubes containing 1-mL ice-cold saline. These samples were then centrifuged at 14,000 rpm for 2 minutes to produce cell pellets, the supernatant was aspirated, and the remaining pellets were carefully washed with 0.5- to 1.0-mL ice-cold saline to remove remaining unbound MIBI. The sample radioactivity was counted using an automatic γ counter (WIZARD "3" 1480; Perkin Elmer, Life Science). The accumulation ratio (CPM_{in}/CPM_{out}) was calculated as the ratio of radioactivity concentration inside the cell to that found in the supernatant. Using the measurements of radioactivity in the cell pellets and a standard representing the supernatant concentration together with an independent measurement of cell volume, the accumulation ratio equation was calculated as follows (24, 25):

$$CPM_{in}/CPM_{out} = \frac{\text{counts per minute}_{pellet} \times \#\text{cells}_{pellet}}{\text{counts per minute}_{supernatant}}$$

where $\text{counts per minute}_{pellet}$ is the measured radioactivity rate of the pellet, $\text{counts per minute}_{supernatant}$ is the measured radioactivity rate of the supernatant, $\text{volume}_{pellet} = \text{volume}_{supernatant} = 300$ μL, and $\#\text{cells}_{pellet} = \text{volume}_{pellet} \times \text{density}_{pellet} = 300\ \mu L \times (5 \times 10^5\ \text{cells}/\mu L)^*$ (* is the constant density per 0.1 mL of packed H1299 cells).

The CPM_{in}/CPM_{out} ratios of the I and C groups were measured at 60 minutes after the addition of MIBI. These MIBI accumulation studies were repeated four times.

The correlation study

We analyzed the correlation between cell multiplication and MDR using the RC from the *in vitro* replication study and the accumulation ratios from the *in vivo* MIBI accumulation study.

Doxorubicin fluorescence imaging study *in vivo*

This animal study obtained approval from an appropriate animal care committee in conformance with the Guide for the Care and Use of Laboratory Animals [Institute for Laboratory Animal Research (ILAR) 8th Edition, 2010].

Approximately 5.0 million human non–small lung cancer cells, from the same line (H1299), were subcutaneously inoculated into a BALB/c-nu/nu mouse model at the dorsal right shoulder. The tumors were grown until they attained a volume of at least 75 mm^3. Five such mice were prepared as irradiation-free controls and another five were prepared for localized thoracic irradiation. The irradiated mice received a total γ-ray dose of 9 Gy via a lead shield collimated ^{137}Cs source (Gammacell 40 Exactor; Nordion International). At 7 days after 9-Gy irradiation, 200 μg/100 μL of doxorubicin was injected into the tail veins of both the control and irradiated mice. Doxorubicin accumulation (counts/mm^3) was measured from injection to 1, 60, and 120 minutes after injection using an *in vivo* fluorescent imaging system (Xenogen-IVIS Lumina; PerkinElmer Inc.). The doxorubicin accumulation ratio, $AR_{doxorubicin}$, was defined as the ratio of the irradiated region of interest, ROI_{IR}, normalized by a nonirradiated region of interest, ROI_{NIR}, thus

$$AR_{doxorubicin} = \frac{ROI_{IR}}{ROI_{NIR}}.$$

Specifically, ROI_{IR} was defined as a circular region, with a diameter of 6 mm, at the tumor mass of the irradiated site, and ROI_{NIR} was similarly defined as a circular region, with a diameter of 18 mm, at the skin of the shielded site. The doxorubicin accumulation ratios of the irradiated groups were compared with the control group.

Statistical analysis and the correlation study

The statistical analyses of the results of the *in vitro* replication and MIBI accumulation studies and the *in vivo* doxorubicin fluorescent imaging study were all performed using repeated ANOVA. The correlation between the *in vitro* cell replication and MIBI accumulation studies was determined using the linear Spearman rank correlation coefficient. The threshold for statistical significance for all statistical analyses was set as $P < 0.05$.

Results

Replication study *in vitro*

Irradiation suppressed the cell RR in all the I groups relative to the C group. This RR suppression was found to be dose dependent, over the entire time interval of observation from 1 to 14 days. Although the RR decreased after irradiation, the cells continued to multiply in all I groups with the exception of the 12-Gy (high dose) I group (Fig. 2). In Table 1, the RC of all the I groups is compared with that of the C group. In 1 day after irradiation, no statistically significant difference for the RC was found relative to the C group. Besides, for all I groups,

Published OnlineFirst August 20, 2014; DOI: 10.1158/1535-7163.MCT-14-0151

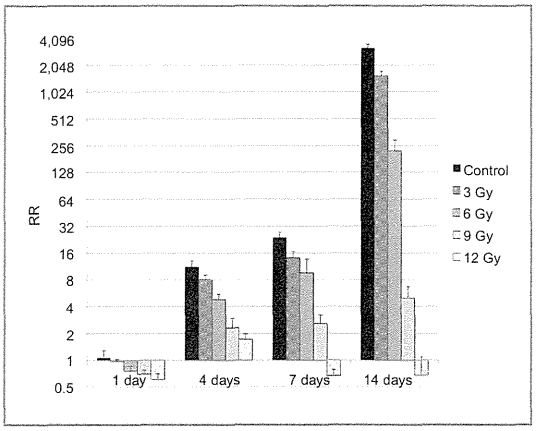

Figure 2. The RRs of the H1299 cell line control group and each of the H1299 irradiation groups. Error bars, mean ± SD; $n = 4$.

a significant RC dose-dependent decline was found from 4 to 14 days after irradiation.

Tc-99m MIBI accumulation study *in vitro*

Intracellular MIBI accumulation was observed, for both the C group and all I groups, after MIBI addition. The CPM_{in}/CPM_{out} ratio attained a plateau at about 30 minutes after the addition of MIBI (45- and 60-minute data were within ± SE) in all groups. A dose-dependent increase in the CPM_{in}/CPM_{out} ratio, indicating increased intracellular MIBI uptake, was observed from 4 to 14 days after irradiation in all the I groups (Fig. 3A). The graph consisting of 60-minute data of all periods (Fig. 3B) shows the time-dependent effect of inhibition of MDR by irradiation. Using this result, the CPM_{in}/CPM_{out} ratio at 60 minutes after addition of MIBI was measured from 4 to 14 days for both the C and I groups to determine the longitudinal time effect of irradiation on MDR (Fig. 3B). For both the C group and 3-Gy I group, no statistically significant difference in MIBI accumulation was observed from 1 to 14 days after irradiation. For the 9- and 12-Gy I groups, a statistically significant higher CPM_{in}/CPM_{out} ratio was observed from 4 to 14 days after irradiation compared with the C group. For the 6-Gy I group, a significantly higher CPM_{in}/CPM_{out} ratio was observed at the 7th day. However, unlike the 9-Gy I group, there was no significant difference at the 14th day. Suppression of MDR was thus found to be irradiation dose dependent.

Correlation study *in vitro*

The Spearman rank correlation coefficient analysis found a statistically significant negative correlation between CPM_{in}/CPM_{out} and RC (Fig. 4).

Doxorubicin fluorescent imaging *in vivo*

In both the C group and 9-Gy I group, whole mouse body fluorescence increased, after doxorubicin injection, for the first 10 minutes. After 10 minutes, whole body fluorescence slowly decreased until the measurement endpoint at 120 minutes after injection. At 1 minute after injection, a similar accumulation of doxorubicin was observed in both the C group and the 9-Gy I group. On the other hand, at 60 and 120 minutes, a large accumulation of doxorubicin was observed at the irradiated site of the 9-Gy I group. A statistically significant higher $AR_{doxorubicin}$ was found in the 9-Gy I group at 60 and 120 minutes after injection relative to the C group (Figs. 5 and 6).

Discussion

The *in vitro* cell replication study demonstrated the non–small lung cancer cell line H1299/wtp53 sensitivity to γ-ray irradiation. Dose-dependent inhibition of cell replication was observed in all the groups subject to γ-irradiation. The largest inhibition was observed in 7 days after irradiation. The most probable cause is DNA damage. Furthermore, it was found that this cancer cell line was resilient to single-dose irradiation, even at the 12-Gy high dose, as demonstrated by the recovery of replication capacity of the irradiated cells after the 14 days.

Table 1. The replication coefficient

RC	1 day	4 days	7 days	14 days
Control (0 Gy)	−0.06 (0.50)	0.87 (0.06)	0.65 (0.03)	0.83 (0.01)
3 Gy	−0.06 (0.15)	0.75 (0.04)[a]	0.54 (0.04)[a]	0.76 (0.01)[a]
6 Gy	−0.27 (0.33)	0.56 (0.05)[a]	0.45 (0.10)[a]	0.55 (0.03)[a]
9 Gy	−0.26 (0.47)	0.29 (0.08)[a]	0.19 (0.05)[a]	0.16 (0.03)[a]
12 Gy	−0.29 (0.22)	0.19 (0.05)[a]	−0.09 (0.04)[a]	−0.09 (0.10)[a]

NOTE: Significance testing was done using the pairwise Mann–Whitney *U* test. Significant difference between control (0 Gy) and other irradiated groups.

[a]$P < 0.05$. Values are expressed as mean (SD); $n = 4$.

Published OnlineFirst August 20, 2014; DOI: 10.1158/1535-7163.MCT-14-0151

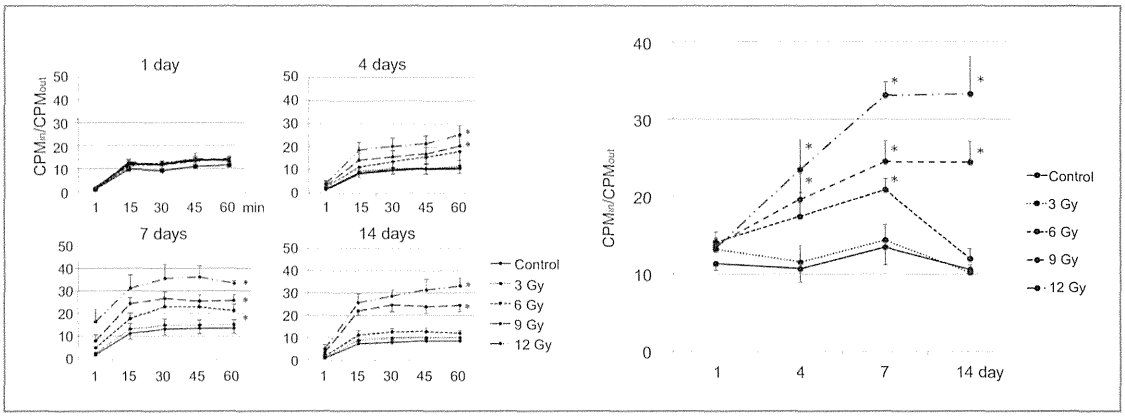

Figure 3. A, the CPM_{in}/CPM_{out} of the control group and each of the irradiation groups. These groups displayed the number of days after irradiation. The transverse shows CPM_{in}/CPM_{out} ratio. B, CPM_{in}/CPM_{out} at 60 minutes after the addition of MIBI for 1, 4, 7, and 14 days after irradiation. *, $P < 0.05$. Bars, mean ± SE; $n = 4$.

The effect of γ-irradiation on MDR in H1299/wtp53 was investigated using Tc-99m MIBI. MIBI, with similar pharmacokinetics to chemotherapeutic drugs such as doxorubicin, is known to be a substrate of the overexpressed ABC transporters responsible for MDR in cancer cells. Therefore, suppression of MDR via irradiation can be effectively investigated using the change in intracellular uptake of MIBI. Furthermore, based on this pharmacokinetic property, a number of clinical studies have reported that MIBI imaging may be used to obtain an early estimate of the therapeutic response to chemotherapy by assessing the cancer MDR (16–23). In this study, MIBI was used to investigate the response of MDR in H1299/*wtp53 in vitro*. The increase in intracellular MIBI retention that was observed from the 4 to 14 days after irradiation is evidence for the suppression of MDR in H1299/*wtp53* due to γ-irradiation. Furthermore, the amount and duration of MDR suppression were found to be γ-irradiation dose dependent, a finding that we suggest may be important for clinical chemoradiotherapy. Finally, these *in vitro* results are further supported by the *in vivo* result, obtained via fluorescent imaging in a mouse model, that MDR to the uptake of the chemotherapeutic agent doxorubicin is suppressed by γ-irradiation. This result can be considered as additional evidence for the *in vivo* suppression of MDR by γ-irradiation in the non–small lung cancer cell line H1299/*wtp53*.

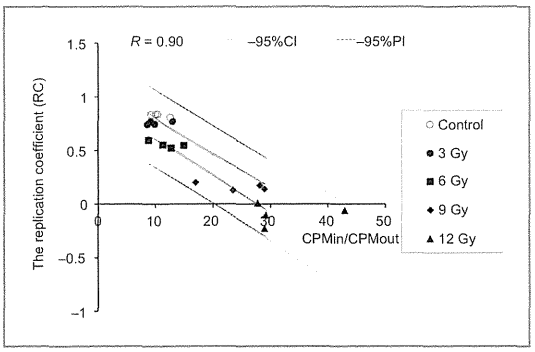

Figure 4. The correlation between RC and CPM_{in}/CPM_{out} at 14 days after irradiation. We evaluated this relationship between cell multiplication and MDR using the Spearman correlation coefficient. A significant negative correlation between RC and CPM_{in}/CPM_{out} was found.

The molecular basis of the effect of irradiation on MDR is not yet clear. Xie and colleagues (9) have reported that fractionated irradiation-induced radioresistant esophageal cancer cells are more sensitive to certain types of chemotherapeutic drugs, including doxorubicin. Our study extends prior reports of MDR suppression by irradiation. Conversely, it has also been reported that irradiated cancer cells can develop resistance to chemotherapy. Overexpression of ABC transporters associated with MDR has been observed in human cancer cell lines after irradiation (26, 27). Bottke and colleagues (11) have reported that irradiation can induce functionally relevant MDR gene and protein expression. Thus, further research is clearly required to elucidate the molecular basis of the response of different cancer cell lines to radiotherapy with regard to MDR.

This study focused on MDR in cancer cells over the short-time interval of 14 days immediately after γ-irradiation. MDR suppression due to γ-irradiation was observed, both *in vitro* and *in vivo*, over this short interval during which non–small lung cancer cell replication was also reduced. This set of results provides additional experimental evidence in support of the synergistic efficacy of chemoradiotherapy as reported by clinical studies (4–8). The movement of

Published OnlineFirst August 20, 2014; DOI: 10.1158/1535-7163.MCT-14-0151

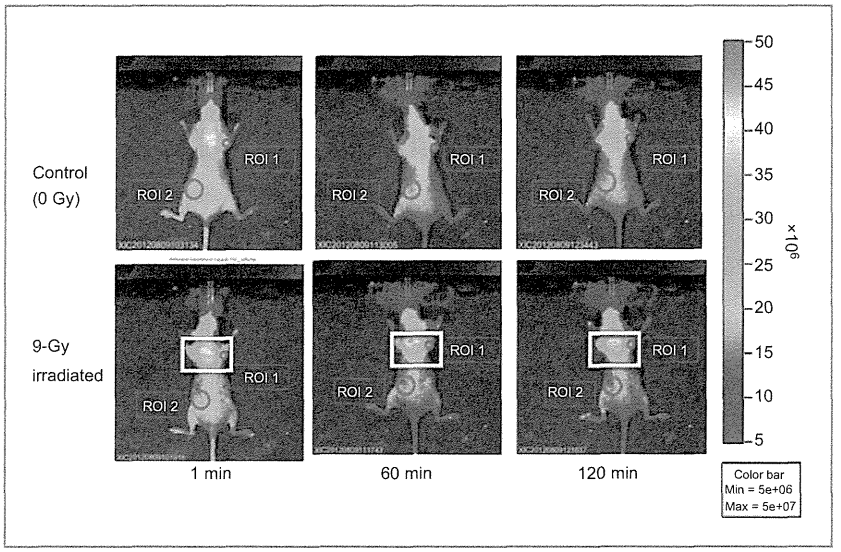

Figure 5. Doxorubicin fluorescent imaging. Top, images from the control group (0 Gy). Bottom, images from the 9-Gy irradiation group. Doxorubicin accumulation in the 9-Gy group was observed at the irradiated site, the region enclosed by the white square line.

MIBI across the cell membrane for influx is passive transport by diffusion and for efflux is active transport by the ABC transporters which are overexpressed in cancer cells resulting in MDR. The current hypothesis is that γ-irradiation disrupts, in some manner, the cellular active transport process. However, to date, to the best of our knowledge, no studies have been published with regard to this hypothesis. In this article, we did not investigate how the underlying molecular mechanisms are affected by γ-irradiation. However, based on the negative correlation between cancer cell replication and MIBI accumulation, we suggest that γ-irradiation may cause MDR-related protein damage or suppression of the active transporter's metabolic function.

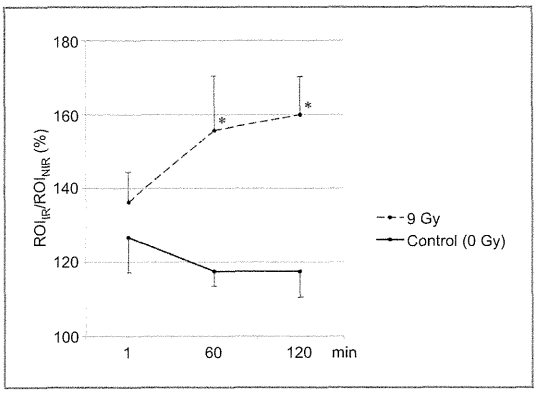

Figure 6. The ROI_{IR}/ROI_{NIR} in doxorubicin fluorescent imaging. *, $P < 0.05$. Values expressed as mean (SD); $n = 5$.

Conclusion

MDR in the non–small lung cancer cell line H1299/*wtp53* was suppressed after γ-irradiation. The amount and duration of the suppression depended on the γ-irradiation dose. A statistically significant negative correlation was found between cell replication and MDR suppression after γ-irradiation in this cell line.

Disclosure of Potential Conflicts of Interest

No potential conflicts of interest were disclosed.

Authors' Contributions

Conception and design: Y. Kono, K. Utsunomiya
Development of methodology: Y. Kono, K. Utsunomiya
Acquisition of data (provided animals, acquired and managed patients, provided facilities, etc.): Y. Kono, K. Utsunomiya
Analysis and interpretation of data (e.g., statistical analysis, biostatistics, computational analysis): Y. Kono, K. Utsunomiya
Writing, review, and/or revision of the manuscript: Y. Kono, K. Utsunomiya
Administrative, technical, or material support (i.e., reporting or organizing data, constructing databases): Y. Kono, K. Utsunomiya, S. Kanno
Study supervision: K. Utsunomiya, N. Tanigawa

Acknowledgments

The authors thank Dr. Hideki Matsumoto (Division of Oncology, Biomedical Imaging Research Center, Fukui University, Japan) for kindly providing the human non–small lung cancer cells (H1299) used in this study, Audrius Stundzia, Ph.D., Tomographix IP Ltd., for valuable advice about this article, and Professor Ralph McCready (Royal Sussex County Hospital, Brighton, United Kingdom) for his evaluation of this study. Finally, the authors thank the two anonymous reviewers for their constructive criticisms and suggestions.

The costs of publication of this article were defrayed in part by the payment of page charges. This article must therefore be hereby marked *advertisement* in accordance with 18 U.S.C. Section 1734 solely to indicate this fact.

Received February 21, 2014; revised August 7, 2014; accepted August 8, 2014; published OnlineFirst August 20, 2014.

Published OnlineFirst August 20, 2014; DOI: 10.1158/1535-7163.MCT-14-0151

References

1. Palmeira A, Sousa E, Vasconcelos MH, Pinto MM. Three decades of P-gp inhibitors: skimming through several generations and scaffolds. Curr Med Chem 2012;19:1946–2025.
2. Chou PM, Reyes-Mugica M, Barquin N, Yasuda T, Tan X, Tomita T. Multidrug resistance gene expression in childhood medulloblastoma: correlation with clinical outcome and DNA ploidy in 29 patients. Pediatr Neurosurg 1995;23:283–91; discussion 91–2.
3. Lee SH, Kim H, Hwang JH, Lee HS, Cho JY, Yoon YS, et al. Breast cancer resistance protein expression is associated with early recurrence and decreased survival in resectable pancreatic cancer patients. Pathol Int 2012;62:167–75.
4. Pignon JP, Bourhis J, Domenge C, Designe L. Chemotherapy added to locoregional treatment for head and neck squamous-cell carcinoma: three meta-analyses of updated individual data. MACH-NC Collaborative Group. Meta-analysis of chemotherapy on head and neck cancer. Lancet 2000;355:949–55.
5. al-Sarraf M, Martz K, Herskovic A, Leichman L, Brindle JS, Vaitkevicius VK, et al. Progress report of combined chemoradiotherapy versus radiotherapy alone in patients with esophageal cancer: an intergroup study. J Clin Oncol 1997;15:277–84.
6. Green JA, Kirwan JM, Tierney JF, Symonds P, Fresco L, Collingwood M, et al. Survival and recurrence after concomitant chemotherapy and radiotherapy for cancer of the uterine cervix: a systematic review and meta-analysis. Lancet 2001;358:781–6.
7. Fukuoka M, Furuse K, Saijo N, Nishiwaki Y, Ikegami H, Tamura T, et al. Randomized trial of cyclophosphamide, doxorubicin, and vincristine versus cisplatin and etoposide versus alternation of these regimens in small-cell lung cancer. J Natl Cancer Inst 1991; 83:855–61.
8. Nishimura Y. Rationale for chemoradiotherapy. Int J Clin Oncol 2004;9:414–20.
9. Xie L, Song X, Yu J, Wei L, Song B, Wang X, et al. Fractionated irradiation induced radio-resistant esophageal cancer EC109 cells seem to be more sensitive to chemotherapeutic drugs. J Exp Clin Cancer Res 2009;28:68.
10. Ryu JS, Um JH, Kang CD, Bae JH, Kim DU, Lee YJ, et al. Fractionated irradiation leads to restoration of drug sensitivity in MDR cells that correlates with down-regulation of P-gp and DNA-dependent protein kinase activity. Radiat Res 2004;162:527–35.
11. Bottke D, Koychev D, Busse A, Heufelder K, Wiegel T, Thiel E, et al. Fractionated irradiation can induce functionally relevant multidrug resistance gene and protein expression in human tumor cell lines. Radiat Res 2008;170:41–8.
12. Piwnica-Worms D, Chiu ML, Budding M, Kronauge JF, Kramer RA, Croop JM. Functional imaging of multidrug-resistant P-glycoprotein with an organotechnetium complex. Cancer Res 1993;53: 977–84.
13. Fonti R, Del Vecchio S, Zannetti A, De Renzo A, Catalano L, Pace L, et al. Functional imaging of multidrug resistant phenotype by 99mTc-MIBI scan in patients with multiple myeloma. Cancer Biother Radiopharm 2004;19:165–70.
14. Gomes CM, Abrunhosa AJ, Pauwels EK, Botelho MF. P-glycoprotein versus MRP1 on transport kinetics of cationic lipophilic substrates: a comparative study using [99mTc]sestamibi and [99mTc]tetrofosmin. Cancer Biother Radiopharm 2009;24:215–27.
15. Yuksel M, Cermik TF, Doganay L, Karlikaya C, Cakir E, Salan A, et al. 99mTc-MIBI SPET in non-small cell lung cancer in relationship with Pgp and prognosis. Eur J Nucl Med Mol Imaging 2002;29:876–81.
16. Kao A, Shiun SC, Hsu NY, Sun SS, Lee CC, Lin CC. Technetium-99m methoxyisobutylisonitrile chest imaging for small-cell lung cancer. Relationship to chemotherapy response (six courses of combination of cisplatin and etoposide) and p-glycoprotein or multidrug resistance related protein expression. Ann Oncol 2001;12:1561–6.
17. Nishiyama Y, Yamamoto Y, Satoh K, Ohkawa M, Kameyama K, Hayashi E, et al. Comparative study of Tc-99m MIBI and Tl-201 SPECT in predicting chemotherapeutic response in non-small-cell lung cancer. Clin Nucl Med 2000;25:364–9.
18. Yuksel M, Cermik TF, Karlikaya C, Salan A, Cakir E, Gultekin A, et al. Monitoring the chemotherapeutic response in primary lung cancer using 99mTc-MIBI SPET. Eur J Nucl Med 2001;28:799–806.
19. Kao CH, ChangLai SP, Chieng PU, Yen TC. Technetium-99m methoxyisobutylisonitrile chest imaging of small cell lung carcinoma: relation to patient prognosis and chemotherapy response–a preliminary report. Cancer 1998;83:64–8.
20. Yamamoto Y, Nishiyama Y, Fukunaga K, Satoh K, Fujita J, Ohkawa M. 99mTc-MIBI SPECT in small cell lung cancer patients before chemotherapy and after unresponsive chemotherapy. Ann Nucl Med 2001;15:329–35.
21. Shih CM, Hsu WH, Huang WT, Wang JJ, Ho ST, Kao A. Usefulness of chest single photon emission computed tomography with technetium-99m methoxyisobutylisonitrile to predict taxol based chemotherapy response in advanced non-small cell lung cancer. Cancer Lett 2003;199:99–105.
22. Akgun A, Cok G, Karapolat I, Goksel T, Burak Z. Tc-99m MIBI SPECT in prediction of prognosis in patients with small cell lung cancer. Ann Nucl Med 2006;20:269–75.
23. Mohan HK, Miles KA. Cost-effectiveness of 99mTc-sestamibi in predicting response to chemotherapy in patients with lung cancer: systematic review and meta-analysis. J Nucl Med 2009;50:376–81.
24. Ballinger JR, Hua HA, Berry BW, Firby P, Boxen I. 99Tcm-sestamibi as an agent for imaging P-glycoprotein-mediated multi-drug resistance: in vitro and in vivo studies in a rat breast tumour cell line and its doxorubicin-resistant variant. Nucl Med Commun 1995;16:253–7.
25. Ballinger JR, Bannerman J, Boxen I, Firby P, Hartman NG, Moore MJ. Technetium-99m-tetrofosmin as a substrate for P-glycoprotein: in vitro studies in multidrug-resistant breast tumor cells. J Nucl Med 1996;37:1578–82.
26. Hill BT, Moran E, Etievant C, Perrin D, Masterson A, Larkin A, et al. Low-dose twice-daily fractionated X-irradiation of ovarian tumor cells in vitro generates drug-resistant cells overexpressing two multidrug resistance-associated proteins, P-glycoprotein and MRP1. Anticancer Drugs 2000;11:193–200.
27. Nielsen D, Maare C, Eriksen J, Litman T, Skovsgaard T. Expression of P-glycoprotein and multidrug resistance associated protein in Ehrlich ascites tumor cells after fractionated irradiation. Int J Radiat Oncol Biol Phys 2001;51:1050–7.

Published OnlineFirst August 20, 2014; DOI: 10.1158/1535-7163.MCT-14-0151

AACR American Association for Cancer Research

Molecular Cancer Therapeutics

Longitudinal Time-Dependent Effects of Irradiation on Multidrug Resistance in a Non–Small Lung Cancer Cell Line

Yumiko Kono, Keita Utsunomiya, Shohei Kanno, et al.

Mol Cancer Ther 2014;13:2706-2712. Published OnlineFirst August 20, 2014.

CLINICAL STUDY

Radiation Dose of Nurses during IR Procedures: A Controlled Trial Evaluating Operator Alerts before Nursing Tasks

Atsushi Komemushi, MD, PhD, Satoshi Suzuki, MD, Akira Sano, MD, PhD, Shohei Kanno, MD, Shuji Kariya, MD, PhD, Miyuki Nakatani, MD, Rie Yoshida, MD, Yumiko Kono, MD, Koshi Ikeda, MD, PhD, Keita Utsunomiya, MD, PhD, Yoko Harima, MD, PhD, Sadao Komemushi, PhD, and Noboru Tanigawa, MD, PhD

ABSTRACT

Purpose: To compare radiation exposure of nurses when performing nursing tasks associated with interventional procedures depending on whether or not the nurses called out to the operator before approaching the patient.

Materials and Methods: In a prospective study, 93 interventional radiology procedures were randomly divided into a call group and a no-call group; there were 50 procedures in the call group and 43 procedures in the no-call group. Two monitoring badges were used to calculate effective dose of nurses. In the call group, the nurse first told the operator she was going to approach the patient each time she was about to do so. In the no-call group, the nurse did not say anything to the operator when she was about to approach the patient.

Results: In all the nursing tasks, the equivalent dose at the umbilical level inside the lead apron was below the detectable limit. The equivalent dose at the sternal level outside the lead apron was 0.16 μSv ± 0.41 per procedure in the call group and 0.51 μSv ± 1.17 per procedure in the no-call group. The effective dose was 0.018 μSv ± 0.04 per procedure in the call group and 0.056 μSv ± 0.129 per procedure in the no-call group. The call group had a significantly lower radiation dose ($P = .034$).

Conclusions: Radiation doses of nurses were lower in the group in which the nurse called to the operator before she approached the patient.

ABBREVIATIONS

H_a = 1-cm dose equivalent at the sternal level on the outside of the lead apron, H_b = 1-cm dose equivalent at the umbilical level inside the lead apron, H_E = effective dose of nonuniform exposure ($H_E = 0.11\ H_a + 0.89\ H_b$)

Komemushi et al (1) prospectively investigated the radiaion dose in nursing tasks associated with interventional radiology procedures, and they reported that the effective dose per procedure was 0.14 μSv. Radiation exposure of nurses in interventional radiology procedures is mainly accounted for by the exposure that occurs when approaching patients during fluoroscopy. If nurses call out to the operator before approaching the patient, the operator can potentially halt the fluoroscopy and reduce unnecessary exposure to nurses. The aim of this study was to compare nurses' exposure when performing nursing tasks associated with interventional radiology procedures depending on whether or not the nurses called out to the operator before approaching the patient.

MATERIALS AND METHODS

This study was approved by the Ethics Committee of the authors' institution. All patients and all nurses provided

From the Department of Radiology (A.K., S.S., A.S., S.Kan., S.Kar., M.N., R.Y., Y.K., K.I., K.U., Y.H., N.T.), Kansai Medical University, 10-15, Fumizono, Moriguchi, Osaka, 570-8507 Japan; and Graduate School of Engineering (S.Ko.), Osaka City University, Osaka, Japan. Received January 24, 2014; final revision received and accepted March 17, 2014. Address correspondence to A.K.; E-mail: kome64@yo.rim.or.jp

None of the authors have identified a conflict of interest.

J Vasc Interv Radiol 2014; 25:1195–1199

http://dx.doi.org/10.1016/j.jvir.2014.03.021

their written informed consent. All nursing tasks in interventional radiology procedures were performed under the management of a radiation protection subchief at the authors' institution who held a First Class Radiation Protection Supervisor qualification. This study was registered with University Hospital Medical Information Clinical Trials Registry (UMIN000012328).

Sample Size

The sample size needed to evaluate radiation dose when comparing the mean values of continuous variables that conformed to a normal distribution in the two groups being tested using Student *t* test, assuming a mean value of $\mu 1 = 0.5$ in the control group, $\mu 2 = 0.1$ in the comparison group, and SD $\sigma = 0.5$, and taking $\alpha = .05$ and power = 80%, was $n = 26$ in the control group and $n = 26$ in the comparison group, for a total sample size of $n = 52$. In our institution, the number of procedures in a typical month is 30, and so the study duration was set at 3 months to ensure a sufficient number of patients, anticipating variation in the number of procedures and protocol divergence. All nurses participating in this study were women.

All nursing tasks during interventional radiology procedures performed in our hospital during the period from March through May 2012 were investigated. Interventional radiology procedures were randomly divided into a call group (in which the nurse called to the operator before approaching the patient) and a no-call group. The randomized allocation sequence was concealed from all nursing staff until interventions were assigned. The random allocation sequence was generated by computer software (Microsoft Excel 2010; Microsoft Japan Co, Ltd, Tokyo, Japan). A.K. enrolled participants and assigned participants to interventions.

Radiation doses during nursing tasks were measured for all nurses engaged in nursing procedures. Radiation doses of operators were also measured. In the call group, the nurse first told the operator she was going to approach the patient each time she was about to do so. In the no-call group, the nurse did not say anything to the operator when she was about to approach the patient. For each interventional radiology procedure, the name of the procedure and the fluoroscopy time were recorded.

When engaged in interventional radiology procedure nursing tasks, the nurses wore radiation protective lead aprons (lead equivalent, 0.25 mm Pb) (LO-S; Hosina Co, Tokyo, Japan). Electronic pocket radiation dosimeters (PDM-117; Aloka Co, Ltd, Tokyo, Japan) were attached at the sternal level on the outside of the radiation protective lead apron and at the umbilical level inside the apron (Fig 1). The parameters of the electronic pocket radiation dosimeters were as follows: energy threshold, 20 keV; detector, silicon solid-state; energy response, 30 keV to 3 MeV within ±30% (calibrated by 40 keV of x-rays using a slab phantom); accuracy, within ±20% (10–9,999 μSv) (calibrated by 40

Figure 1. Radiation dose measurement. Radiation doses were measured using electronic personal dosimeters attached on the outside at the sternal level and inside at the umbilical level of lead aprons. The doses were assessed in terms of equivalent dose penetrating at 10-mm tissue depth outside (H_a) and inside the lead apron (H_b).

keV of x-rays using a slab phantom); linearity, within ±10% (up to 30 mSv/h), within ±20% (30–100 mSv/hour), complying with International Commission on Radiological Protection Publication No. 74. At the completion of the nursing tasks for each procedure, the measured values of the electronic pocket radiation dosimeters for the 1-cm dose equivalent at the sternal level on the outside of the lead apron (H_a) and the 1-cm dose equivalent at the umbilical level inside the lead apron (H_b) were recorded. Based on the 1990 recommendations of the International Commission on Radiological Protection (2), the effective dose (H_E) was calculated using the formula $H_E = 0.11\ H_a + 0.89\ H_b$ for calculating H_E related to external exposure when exposure is nonuniform (3,4).

The nursing tasks performed in interventional radiology procedures included helping the patient to move, sterilizing puncture sites, observing patient condition, recording vital signs and the progress of the procedure, handing sterilized devices and medical agents to the operator, managing drip infusions, and administering intravenous medical agents. During fluoroscopy, nursing tasks that required the nurse to approach the patient were avoided as much as possible. A workbench for nurses was set up in the examination room, and the recording tasks were done on this workbench. As a rule, nursing tasks during procedures were done in the examination room, but nurses left the examination room during digital radiography and computed tomography (CT) scans. Figure 2 shows the layout of the examination room. No protective screen was set up between the x-ray tubes and workbench. The nurses' workbench was arranged so that their standard work position was on a straight line with the x-ray tubes and operator. Even when the operator moved away from a straight line with the x-ray tubes and workbench, the spatial dose at the nurses' workbench was ≤ 0.1 μSv/min during radioscopy.

IR Procedure

Four physicians performed the examinations: a part-time board-certified interventional radiologist who had been a licensed physician for 39 years, a full-time board-certified interventional radiologist who had been a licensed physician for 15 years, a full-time radiologist who had been a licensed physician for 9 years, and a part-time emergency medicine physician who had been a licensed physician for 12 years. All of these physicians performed the interventional radiology procedures with due care for radiation protection. All procedures were done under the management of a full-time board-certified interventional radiologist who had been a licensed physician for 15 years.

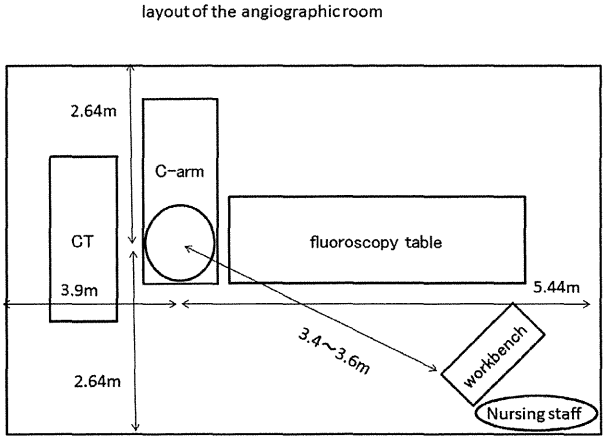

Figure 2. Layout of the angiographic room.

All interventional procedures were performed under a unified CT and angiography system (Advantx-ACT; GE Healthcare, Milwaukee, Wisconsin), which combines angiographic equipment (Advantx-LCA+; GE Healthcare) and CT equipment (HiSpeed LX/i; GE Healthcare) with a single fluoroscopy table (Omega 4 Angio Step; GE Healthcare). The system was not equipped with a CT fluoroscopy function. A movable x-ray protective shield was used to protect the physician performing the procedure from scattered radiation from the patient. The fluoroscopy table was equipped with a protective shield to protect the physician's lower body from scattered radiation. A protective shield to shield the nurse from scattered radiation was not used.

Statistical Analysis

H_a, H_b, H_E, fluoroscopy time, and procedure content were investigated. Bias between the two groups in the procedures was evaluated using χ^2 test. Fluoroscopy time and radiation dose were evaluated with one-way analysis of variance. A P value $< .05$ was considered significant. All analyses were performed using StatView for Windows (Version 5.0; SAS Institute Inc, Cary, North Carolina).

RESULTS

During the study period, 93 procedures were performed. One nurse performed nursing tasks in 79 of 93 procedures, and two nurses performed nursing tasks in 14 of 93 procedures, for a total of 107 nurse-procedures performed. In the call group, 50 procedures and 58 nurse-procedures were performed. In the no-call group, 43 procedures and 49 nurse-procedures were performed. These nursing tasks were performed by five nurses. The radiation doses of nurses and operators were measured in all procedures.

The largest number of interventional radiology procedures involved transarterial treatments for hepatocellular carcinoma. There were no significant differences in the procedures performed in the two groups ($P = .70$) (Table 1).

The fluoroscopy time per procedure was 10.15 min ± 7.5 in the call group and 12.1 min ± 8.3 in the no-call group. There was no significant difference between the groups ($P = .244$) (Table 2).

The operator dose of H_a was 8.88 ± 13.38 μSv/procedure in the call group and 8.79 ± 12.70 μSv/procedure in the no-call group, the operator dose of H_b was 0.48 ± 1.03 μSv/procedure in the call group and 0.65 ± 1.45 μSv/procedure in the no-call group, and the operator dose H_E was 1.40 ± 1.96 μSv/procedure in the call group and 1.55 ± 2.54 μSv/procedure in the no-call group. There were no significant differences between the groups (H_a, $P = .973$; H_b, $P = .509$; H_E, $P = .761$) (Table 2).

In all the nursing tasks, the equivalent dose at the umbilical level inside the radiation protective lead apron (H_b) was below the detectable limit. The equivalent dose at the sternal level outside the lead apron (H_a) was 0.16 ± 0.41 μSv/nurse-procedure in the call group and 0.51 ± 1.17 μSv/nurse-procedure in the no-call group. The radiation dose was significantly lower in the call group ($P = .034$). The effective dose (H_E) with nonuniform exposure was 0.018 ± 0.04 μSv/nurse-procedure in the call group and 0.056 ± 0.129 μSv/nurse-procedure in the no-call group. The call group had a significantly lower radiation dose ($P = .034$) (Table 2). No significant difference was seen in nursing task radiation dose among any of the operators ($P = .172$) or nurses ($P = .571$).

Table 1. Procedures Performed in the Call Group and No-Call Group

	Call Group	No-Call Group
Transarterial chemoembolization/ transarterial infusion	31	28
Angiography	6	8
Trauma of spleen	1	
Trauma of pelvis		1
Vascular stent		1
Balloon angioplasty for dialysis access	1	
Implantation of central venous port catheter system	1	1
Measurement of portal vein pressure	1	
Venous sampling	1	
Biopsy	4	2
Drainage	4	2
Total	50	43
Emergency procedure	3 (6.0%)	2 (4.7%)

DISCUSSION

The dosage rate near the x-ray tubes during fluoroscopy is exceedingly high (5). Most of the radiation exposure during nursing tasks in interventional radiology procedures is thought to occur when the nurse approaches the patient during fluoroscopy. When nurses are going to approach patients, it is thought that if they alert the operator to this beforehand, the operator can halt the fluoroscopy, and unnecessary exposure of nurses can

Table 2. Summary of Results

	Call Group	No-Call Group	ANOVA
Fluoroscopy time (min/procedure)	10.15 ± 7.5 0–29.6 (range) 8.85 (median)	12.1 ± 8.3 0–29.4 (range) 11.4 (median)	$P = .244$
Operator's equivalent dose outside lead apron (H_a) (μSv/procedure)	8.88 ± 13.38 0–72 (range) 4 (median)	8.79 ± 12.70 0–76 (range) 5 (median)	$P = .973$
Operator's equivalent dose inside lead apron (H_b) (μSv/procedure)	0.48 ± 1.03 0–5 (range) 0 (median)	0.65 ± 1.45 0–7 (range) 0 (median)	$P = .509$
Operator's effective dose ($HE = 0.11\ H_a + 0.89\ H_b$) (μSv/procedure)	1.40 ± 1.96 0–8.8 (range) 0.44 (median)	1.55 ± 2.54 0–14.6 (range) 0.66 (median)	$P = .761$
Nurse's equivalent dose outside lead apron (H_a) (μSv/nurse-procedure)	0.16 ± 0.41 0–2 (range) 0 (median)	0.51 ± 1.17 0–6 (range) 0 (median)	$P = .034$
Nurse's equivalent dose inside lead apron (H_b) (μSv/nurse-procedure)	Below detectable limit in all cases	Below detectable limit in all cases	NA
Nurse's effective dose ($H_E = 0.11\ H_a + 0.89\ H_b$) (μSv/nurse-procedure)	0.0176 ± 0.045 0–0.22 (range) 0 (median)	0.0561 ± 0.129 0–0.66 (range) 0 (median)	$P = .034$

ANOVA = analysis of variance; H_a = 1-cm dose equivalent at the sternal level on the outside of the lead apron; H_b = 1-cm dose equivalent at the umbilical level inside the lead apron; H_E = effective dose of nonuniform exposure ($H_E = 0.11\ H_a + 0.89\ H_b$); NA = not applicable.

be reduced. In this study, the radiation dose was significantly lower in nurses in the call group.

Chida et al (6) recommended using two monitoring badges for occupational exposure for interventional radiology procedures. Two monitoring badges were also used in the present study to calculate the effective dose of nurses.

There are differences among reports on radiation doses of nurses. We previously reported that the radiation dose of nurses in interventional radiology procedures was an effective dose of 0.14 μSv/procedure (1). Chida et al (6) reported that the effective dose of nurses in interventional radiology procedures was 1.41 μSv/procedure, and Korir et al (7) reported that the effective dose of nurses in interventional radiology procedures was 30–1,160 μSv/procedure. In this study, the radiation dose of nurses in interventional radiology procedures was much smaller than in past reports in both the call group and the no-call group.

During the study period, the people involved may have had a higher awareness of radiation exposure than usual, and they may have taken more care than usual to protect against radiation exposure. Racadio et al (8) reported that a radiation dose monitoring system that provides real-time feedback to the staff can significantly reduce radiation exposure to the primary operator.

The possible limitations of this study include the following. The study was done with a limited number of operators and a limited number of nurses in a single institution. The measured radiation doses in this study were very low, and it may be that there were exposures below the detectable limit of the measuring instruments that were not measured. Limitations existed in the method of calculating the effective dose used in this study.

In conclusion, a prospective comparison of the radiation dose to nurses when performing nursing tasks associated with interventional procedures depending on whether or not they called to the operator before they approached patients was conducted. Radiation doses of nurses were kept low in the group in which the nurse called to the operator before she approached the patient. Radiation doses of nurses in this study were much lower than in previous studies.

ACKNOWLEDGMENT

This work was supported by Japanese Society for the Promotion of Science KAKENHI Grant Nos. 18790920 and 24791344. The funders had no role in study design, data collection and analysis, decision to publish, or preparation of the manuscript.

The authors thank Ms. Makiko Miyamoto, Dr. Takaya Tsuno, Ms. Yuko Kikukawa, Ms. Noriko Takada, Ms. Tomomi Tojo, Ms. Kazuko Aoki, and Ms. Hanako Matsuoka, whose comments were an enormous contribution to this work.

REFERENCES

1. Komemushi A, Tanigawa N, Aoki A, et al. An observation study of radiation exposure to nurses during interventional radiology procedure. Jpn J Intervent Radiol 2010; 25:470–475.
2. ICRP. 1990 Recommendations of the International Commission on Radiological Protection. ICRP Publication 60. Ann ICRP 1991;21.
3. U.S. Nuclear Regulatory Commission. Regulatory Guide 8.4 Methods for Measuring Effective Dose Equivalent from External Exposure. 2010; 1–8.
4. Komemushi A, Tanigawa N, Kariya S, et al. Radiation exposure to operators during vertebroplasty. J Vasc Interv Radiol 2005; 16:1327–1332.
5. ICRP. Avoidance of radiation injuries from medical interventional procedures. ICRP Publication 85. Ann ICRP 2000;30.
6. Chida K, Kaga Y, Haga Y, et al. Occupational dose in interventional radiology procedures. AJR Am J Roentgenol 2013; 200:138–141.
7. Korir GK, Ochieng BO, Wambani JS, et al. Radiation exposure in interventional procedures. Radiat Prot Dosimetry 2012; 152:339–344.
8. Racadio J, Nachabe R, Carelsen B, et al. Effect of real-time radiation dose feedback on pediatric interventional radiology staff radiation exposure. J Vasc Interv Radiol 2014; 25:119–126.

Cardiovasc Intervent Radiol (2014) 37:1606–1610
DOI 10.1007/s00270-014-0888-z

C RSE

TECHNICAL NOTE

Intranodal Lymphangiogram: Technical Aspects and Findings

Shuji Kariya · Atsushi Komemushi · Miyuki Nakatani · Rie Yoshida · Yumiko Kono · Noboru Tanigawa

Received: 23 August 2013 / Accepted: 23 February 2014 / Published online: 11 April 2014

Abstract
Purpose To report the technical results and imaging findings of intranodal lymphangiogram (INL).
Materials and Methods we studied four patients (three men, one woman) who had persistent chylous leakage despite conservative treatment after esophageal cancer surgery. Their mean age was 68 years (range 61–74 years). The inguinal or femoral lymph node was punctured under ultrasound guidance using a 60-mm-long, 23-gauge needle. If the lipiodol injected via the needle showed granular nodules on fluoroscopy, lipiodol injection was continued manually at a rate of 1 mL/3 min for INL. If the cisterna chyli was detectable on the lymphangiogram, it was punctured percutaneously via the abdomen by a needle under fluoroscopy, and thoracic duct embolization was performed.
Results INL was successful in all patients. Lymphaticovenous anastomoses at the femoral or pelvic region were confirmed in all four patients. In one case, a different ipsilateral lymph node was punctured because major flow of lipiodol into the veins through a lymphaticovenous anastomosis occurred. Catheter cannulation and embolization were successful for three of the four patients. In unsuccessful procedures, the cisterna chyli was not visualized, and puncture was not possible.
Conclusions INL succeeded in all patients. Lipiodol leaked into the vein through a lymphaticovenous anastomosis at the femoral or pelvic region in all patients.

Keywords Chylothorax · Intranodal lymphangiogram · Pulmonary embolization · Thoracic duct embolization

S. Kariya (✉) · A. Komemushi · M. Nakatani · R. Yoshida · Y. Kono · N. Tanigawa
Department of Radiology, Kansai Medical University, 2-5-1 Shinmachi, Hirakata, Osaka 5731010, Japan
e-mail: kariyas@hirakata.kmu.ac.jp

A. Komemushi
e-mail: komemush@takii.kmu.ac.jp

M. Nakatani
e-mail: nakatanm@hirakata.kmu.ac.jp

R. Yoshida
e-mail: yagir@hirakata.kmu.ac.jp

Y. Kono
e-mail: kohnoy@hirakata.kmu.ac.jp

N. Tanigawa
e-mail: tanigano@hirakata.kmu.ac.jp

Introduction

Percutaneous thoracic duct embolization (TDE) using bilateral pedal lymphangiogram for high-output chylothorax was first reported by Cope et al. [1] in 1999. The problem with TDE is that the bilateral pedal lymphangiogram required for this procedure has not been commonly performed in recent years. As a way to overcome this problem, Nadolski and Itkin [2] reported a method of performing TDE using intranodal lymphangiogram (INL). However, there is little information on the technical methods of INL. The objective of this study was to present our technique of INL for TDE.

Materials and Methods

The study protocols for this retrospective analysis were approved by our institutional review board. The requirement for informed consent was waived. Data were gathered

Table 1 Demographic data, treatment before TDE, and volume of effusion drainage

Patient no.	Sex	Age (years)	Conservative treatment			Surgical thoracic duct ligation after conservative treatment		Pre-TDE drainage (mL/day)
			Duration (days)	Pretreatment drainage (mL/day))	Posttreatment drainage (mL/day)	Performed	Postoperative drainage (mL/day)	
1	M	67	166	2,500	1,500	No	–	1,500
2	F	74	30	3,500	2,500	Yes	4,000	4,000
3	M	71	28	2,000	3,000	No	–	3,000
4	M	61	51	600	600	Yes	600	600

TDE thoracic duct embolization

retrospectively by reviewing clinical records, including images.

Patients

The subjects comprised four patients with esophageal cancer. In patients one, two, and three, esophagectomy was performed. In patient four, because cancer progression was confirmed after thoracotomy, esophagectomy was not performed. Three patients (patients one, two, and three) developed high-output chylothorax with daily chest drain output of $\geq$1,000 mL/day after the surgery. One patient (patient four) had chylous leakage of 600 mL/day at the incision site. In patients two and four, a second surgery of thoracic duct (TD) ligation was performed for the chylous leakage. Because chylous leakage persisted despite the second surgery or conservative treatment, TDE was performed in all patients. Table 1 shows the subjects' demographic data, TDE pretreatment, and amount of effusion drainage before and after conservative treatment and TD ligation.

Intranodal Lymphangiogram

A high-frequency (13 MHz) superficial linear transducer and a diagnostic ultrasound device (Prosound 3500SX and UST-5413, Hitachi Aloka Medical, Tokyo, Japan) were used to visualize the lymph nodes. Local anesthesia of the puncture site was administered with 1 % lidocaine; then the inguinal or femoral lymph node was punctured under ultrasound guidance using a 60-mm-long, 23-gauge Cathelin needle (Terumo Europe, Leuven, Belgium). The puncture was made so that the tip of the needle was placed at the junction between the cortex and the hilum. Lipiodol was then injected manually, with the tip of the needle monitored under fluoroscopy (Axiom Artis dTA, Siemens Medical Solutions, Erlangen, Germany) when injection was started. If the injected lipiodol showed granular nodules on fluoroscopy at the start of injection and the lymphatic vessels continuous with them were visualized, the lymph node puncture was judged to be successful, and injection was continued (Fig. 1A). If enhancement of spreading lobulated nodular pooling with no visualization of lymphatic vessels indicated that the puncture was unsuccessful, injection was stopped, and the lymph node was repunctured (Fig. 1B). Lipiodol injection was continued manually at a rate of 1 mL/3 min and stopped at the point at which the lymphatic vessels at the level of the third lumbar vertebra were visualized. During injection, fluoroscopy was used intermittently to confirm that the injected lipiodol was entering the lymphatic vessels. Continuous fluoroscopy was not used to avoid excessive radiation exposure. Leakage of lipiodol from the puncture site was tolerated as long as it was also entering the lymphatic vessels. If there was no flow of lipiodol into the lymphatic vessels despite its injection, puncture was repeated at a different lymph node. The presence of lymphaticovenous anastomoses was confirmed by fluoroscopy. In the event of major flow of lipiodol into the veins through lymphaticovenous anastomoses, injection was halted, and a different ipsilateral lymph node was punctured or only the contralateral lymph node was used for injection.

Transabdominal TDE

Local anesthesia of the skin at the puncture site was achieved with 1 % lidocaine. Antibiotics were not provided. The cisterna chyli was punctured percutaneously via the abdomen by inserting the needle at an angle of approximately 10–20 degrees toward the head under fluoroscopy. A 22-gauge, 20-cm Chiba needle (Angiotech, Gainesville, FL) was used for the puncture. A 0.016-inch wire (Iris, Piolax Medical Devices, Kanagawa, Japan) was inserted and advanced into the TD. A 2.2F microcatheter (Sirabe, Piolax Medical Devices) was advanced into the TD over the wire. Iodinated contrast medium (iopamidol, Iopamiron 370, Bayer Schering Pharma, Berlin, Germany) was manually injected via the catheter for contrast enhancement of the TD. The site of leakage and the location of occlusion of the TD were confirmed. The tip of the

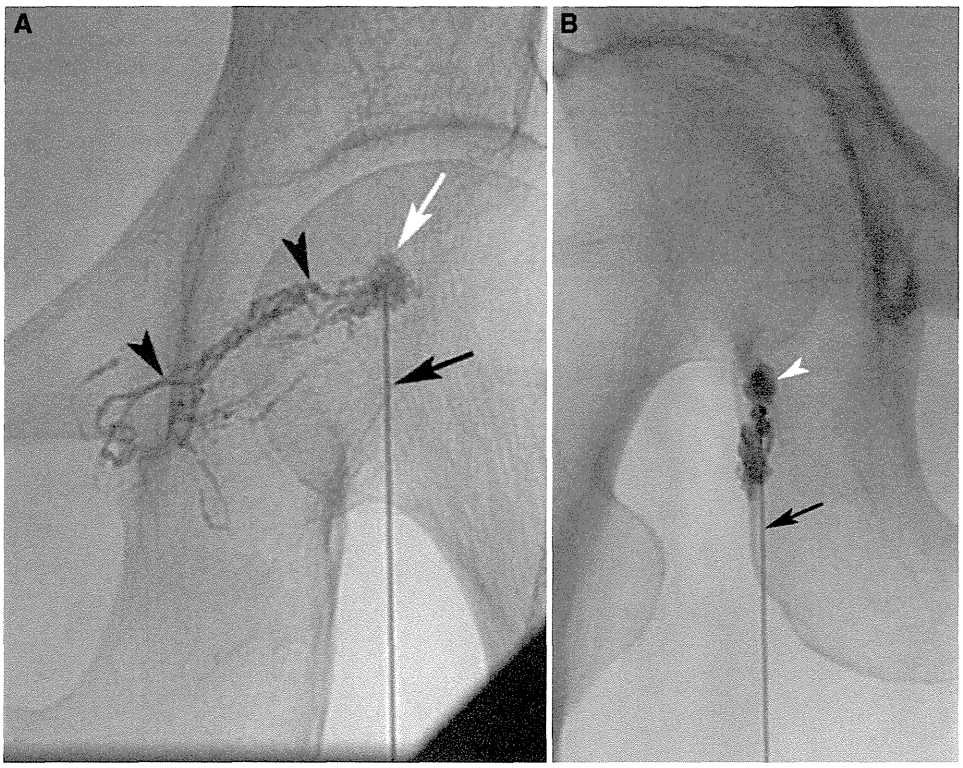

Fig. 1 A 74-year-old woman underwent thoracic duct embolization (TDE) after developing high-output chylothorax after esophagectomy for esophageal cancer. Intranodal lymphangiogram was performed for TDE. **A** Lipiodol is manually injected via the Cathelin needle. The lymph node shows enhancement of the granular nodule (*white arrow*), and the lymphatic vessels continuous with it are detected (*black arrowheads*). Lymph node puncture is successful. Cathelin needle (*black arrow*). **B** A spreading lobulated nodular pooling (*white arrowhead*) with no visualization of lymphatic vessels indicates that lymph node puncture is unsuccessful. Cathelin needle (*black arrow*)

microcatheter was advanced to a position as close as possible to the site of leakage. *N*-Butyl cyanoacrylate (NBCA) mixed with lipiodol was used as the embolization material. Once the NBCA had reached the site of leakage, the TD, cisterna chyli, and puncture route were all embolized with NBCA while the catheter was being withdrawn.

Results

Table 2 shows the results of lymphangiogram. INL was successful in all patients. In patients two and three, the numbers of failed punctures were one and two, respectively. Lymphaticovenous anastomoses at the femoral or pelvic region were confirmed in all four patients. In patient four, a different ipsilateral lymph node was punctured because major flow of lipiodol into the veins through a lymphaticovenous anastomosis occurred (Fig. 2). There were no clinical findings of pulmonary embolization in all four patients. In all patients, continuity between the TD and veins was interrupted as a result of surgical ligation of the TD.

Catheter cannulation and embolization were successful for three of the four patients. In patient three, in whom the cisterna chyli was not visualized, cannulation of the TD was not possible, and TDE was not achieved. In this case, lipiodol drained into the TD via a collateral channel from the lumbar lymphatic vessels.

Discussion

Although over a decade has passed since the first report of TDE, the number of reported TDEs remains relatively low, and the largest series have been reported from a small number of institutions [3, 4]. It has been suggested that this may be due to the technical difficulty involved in lymphangiogram and cannulation of the TD. Bilateral pedal lymphangiogram has been performed with decreasing frequency over the past 20 years, with fewer doctors now able to carry out this procedure, and lymphangiogram pumps are difficult to obtain [5]. INL, which was first reported in 1967, requires neither special equipment nor incisions [6]. There have been few subsequent reports of its use, however, and it has not been generally used for diagnostic lymphangiogram. This may be because of the difficulty of lymph node puncture. This problem may have been solved

Table 2 Results of lymphangiogram

Patient no.	Bilateral lymph node injection	No. of failed lymph node punctures	Total volume of lipiodol injected (mL)	Presence of LVA	Lymphangiography	Complications
1	Successful	0	14	Yes	Successful	No
2	Successful	1	17	Yes	Successful	No
3	Successful	2	10	Yes	Successful	No
4	Successful	0	16	Yes	Successful	No

LVA lymphaticovenous anastomosis

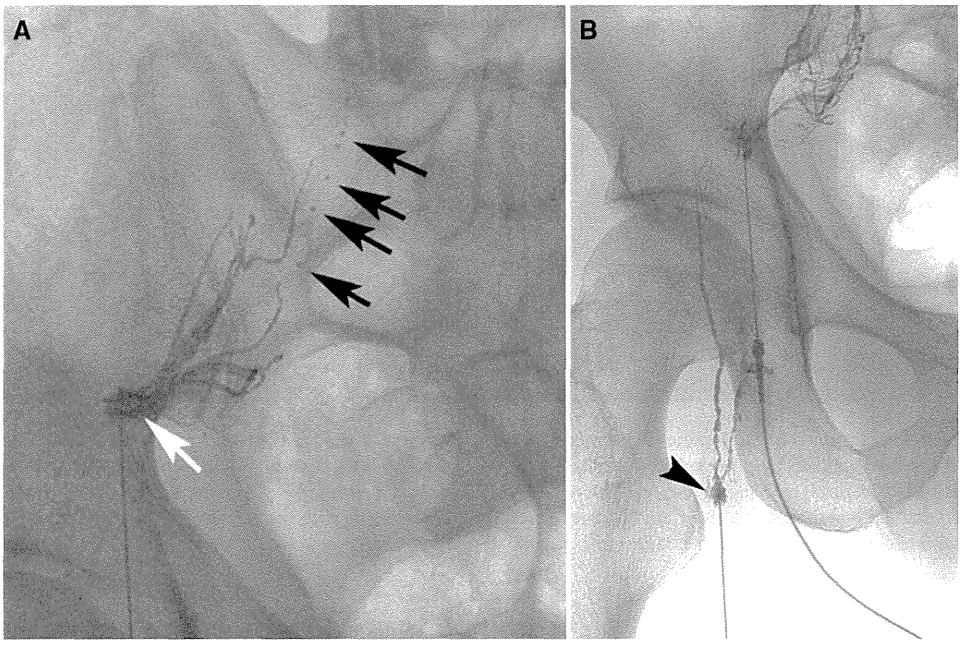

Fig. 2 A 61-year-old man with chylous effusion leakage of 600 mL/day at the incision site after surgery for esophageal cancer. Intranodal lymphangiogram for thoracic duct embolization is performed. **A** The inguinal node (*white arrows*) is punctured, and then lipiodol is injected. Lymphatic vessels are visualized. However, injection is halted because major flow of lipiodol into the veins through lymphaticovenous anastomosis has occurred. *Dots* are lipiodol in the vein (*black arrow*). **B** Another ipsilateral lymph node is punctured (*black arrowhead*)

by the improved performance of the latest ultrasound devices, which enable even impalpable lymph nodes to be punctured under ultrasound guidance. Compared with bilateral pedal lymphangiogram, INL shortens the time required and does not require a lymphangiogram pump [2].

In the present cases, lymphaticovenous anastomoses in the femoral or pelvic region were confirmed in all four patients under fluoroscopy. Peripheral lymphaticovenous anastomoses have also been reported in bilateral pedal lymphangiogram, as has the rare complication of pulmonary embolization [7, 8]. When bilateral pedal lymphangiogram was performed in the past, it is probable that plain X-rays were normally obtained after injection, meaning that lymphaticovenous anastomoses could not be confirmed because still images were obtained. We do not know how much inflow of lipiodol into the veins through lymphaticovenous anastomoses was tolerated, and to our knowledge, it has yet to be reported. With both bilateral pedal lymphangiogram and INL, most of the lipiodol that passes through the TD flows into the veins, and pulmonary oil embolization occurs. When lipiodol leaks into the vein through lymphaticovenous anastomoses, pulmonary oil embolization also occurs. If a lymphaticovenous anastomosis is confirmed, injection of lipiodol might have to be stopped at once to prevent severe pulmonary embolization. However, we did not stop injection. Because some of the injected lipiodol remains in lymph nodes and lymphatic vessels, the amount that actually flows into the veins is unknown. Even so, with lymphangiogram that is normally conducted with $\leq$20 mL of lipiodol, pulmonary oil embolization does not cause symptoms unless respiratory function is severely impaired. We therefore considered the

lipiodol that flowed into veins through lymphaticovenous anastomoses to also be acceptable. However, the safety and tolerance of the leakage of lipiodol into the veins are still unclear. The purpose of INL is to visualize the lymphatic vessels, cisterna chyli, and TD, and this cannot be achieved if much of the lipiodol injected via lymphaticovenous anastomoses flows into the veins. Therefore, injection was stopped when a large amount of lipiodol entered the veins. However, whether to discontinue injection was determined by the operator on the basis of fluoroscopic findings, without any clear criteria.

When lipiodol is injected until the lymphatic vessels at the L3 level are visualized, the amount is sufficient to enable visualization of the cisterna chyli and TD, which is necessary to perform TDE. When lymphatic vessels at the level of L3 are visualized, the cisterna chyli will soon be visualized, and this is a good time to start the TDE procedure. If injection is continued until the cisterna chyli is visualized, lipiodol will pass through the TD before the next TDE, and lipiodol that is not needed to perform the TDE procedure will have been injected.

Lymph node puncture failed three times and was redone. Ultimately, the lymph node puncture was successful in all cases, and INL could be obtained. When puncture fails and a large amount of lipiodol leaks into the area surrounding the lymph nodes, repeat puncture of a lymph node in the same area becomes difficult. It is important to stop injection when fluoroscopic images at the start of lipiodol injection reveal spreading lobulated nodular pooling with no visualization of lymphatic vessels.

Limitation

This study had the limitation that it was a retrospective study involving a small number of patients.

Conclusions

INL succeeded in all patients. Lipiodol leaked into the vein through a lymphaticovenous anastomosis at the femoral or pelvic region in all patients. In 3 of the 4 patients, the cisterna chyli was detected by INL and could be punctured, and TDE was achieved.

Conflict of interest The authors declare that they have no conflict of interest.

References

1. Cope C, Salem R, Kaiser LR (1999) Management of chylothorax by percutaneous catheterization and embolization of the thoracic duct: prospective trial. J Vasc Interv Radiol 10:1248–1254
2. Nadolski GJ, Itkin M (2012) Feasibility of ultrasound-guided intranodal lymphangiogram for thoracic duct embolization. J Vasc Interv Radiol 3:613–616
3. Cope C, Kaiser LR (2002) Management of unremitting chylothorax by percutaneous embolization and blockage of retroperitoneal lymphatic vessels in 42 patients. J Vasc Interv Radiol 13:1139–1148
4. Itkin M, Kucharczuk JC, Kwak A et al (2010) Nonoperative thoracic duct embolization for traumatic thoracic duct leak: experience in 109 patients. J Thorac Cardiovasc Surg 139:584–589
5. Guermazi A, Brice P, Hennequin C et al (2003) Lymphography: an old technique retains its usefulness. Radiographics 23:1541–1558
6. Hall RC, Krementz ET (1967) Lymphangiography by lymph-node injection. JAMA 202:1136–1139
7. Koehler PR, Schaffer B (1967) Peripheral lymphatico-venous anastomoses. Report of two cases. Circulation 35:401–404
8. Takahashi M, Abrams HL (1967) Arborizing pulmonary embolization following lymphangiography. Report of three cases and an experimental study. Radiology 89:633–638